Journal of Carcinogenesis
Covering Genesis to Therapeutics

Journal of Carcinogenesis, ISSN: 1477-3163
2025; Vol 24: Issue 8s, https://carcinogenesis.com/

Indole derivatives in smart polymeric formulations for targeted management of neurodegenerative disorders

Jyothirmayee Devineni[1], Gurinderdeep Singh[2], Dinesh Prabhakar Patil[3], Souvik Sur[4], Abdujabborova Charosxon Sanjarbek qizi[5], Jumanova Barno Ganiyevna[5], Rehana Khanam[6], Iftikhar Ahmed[7], Dhakshnamoorthy Vellingiri[8]*

[1]University College of Pharmaceutical Sciences, Acharya Nagarjuna University, Guntur.

[2]Department of Pharmaceutical Sciences and Drug Research, Punjabi University Patiala, Punjab, India. Address- 45a sheikhpura near Punjabi University Patiala Pincode- 147002.

[3]Mahatma Gandhi Vidyamandir's Samajshri Prashantdada Hiray College of Pharmacy, Malegaon Camp, Loknete Vyankatrao Hiray Marg, Malegaon.

[4]Teerthanker Mahaveer University, Moradabad, Uttar Pradesh-244001, India.

[5]Department of Folk Medicine and Pharmacology, Fergana Medical Institute of Public Health, Fergana-150100, Uzbekistan.

[6]Department of Chemistry, Vidya Bhawan Rural Institute, Udaipur, Rajasthan-313001.

[7]Environmental and Public Health Department, College of Health Sciences, Abu Dhabi University, P.O. Box 59911, Abu Dhabi, United Arab Emirates.

[8]Department of Formulation Research and Development, University of Iowa Pharmaceuticals, College of Pharmacy, University of Iowa, Iowa City, IA, USA.

***Corresponding author:**

Mr. Dhakshnamoorthy Vellingiri,

Department of Formulation Research and Development, University of Iowa Pharmaceuticals, College of Pharmacy,

University of Iowa, Iowa City, IA, USA.

Email ID : dhakshnamoorthy-vellingiri@uiowa.edu

ABSTRACT

Indole derivatives represent a privileged scaffold with multi-target neuroprotective properties (antioxidant, anti-aggregatory, cholinesterase inhibition) but are often limited by poor aqueous solubility, metabolic instability, and restricted brain delivery. In this study, a focused series of indole derivatives was synthesized and characterized. Lead compounds were encapsulated into smart polymeric carriers — (i) ligand-functionalized PEG-PLA nanoparticles for receptor-mediated brain targeting, (ii) disulfide-linked redox-sensitive polymeric micelles for intracellular triggered release, and (iii) thiolated-chitosan intranasal nanogels for nose-to-brain delivery. Formulations were prepared by nanoprecipitation, emulsion–solvent evaporation, and ionotropic gelation respectively, and comprehensively evaluated for particle size, zeta potential, drug loading, encapsulation efficiency, in-vitro release under physiological and stimulus conditions, cytotoxicity, BBB permeation (hCMEC/D3 monolayer and transwell co-culture), and ex vivo brain uptake. Representative indole lead ITD-7 showed high encapsulation (EE 78–86%) and sustained release over 72 h with accelerated release under reductive (10 mM GSH) or acidic (pH 5.5) conditions. Targeted PEG-PLA NPs exhibited ~3.6-fold higher transendothelial transport compared to free ITD-7 and improved neuronal protection in Aβ-challenged SH-SY5Y cells. Thiolated-chitosan nanogels delivered therapeutically relevant drug levels to olfactory bulb tissue in ex vivo rat nasal perfusion studies. These results demonstrate that combining rational indole chemistry with stimulus-responsive, targeted polymeric systems yields promising platforms for targeted management of neurodegenerative disorders

Keywords: *Indole derivatives; smart polymeric formulations; PEG-PLA nanoparticles; redox-sensitive micelles; intranasal nanogel; blood–brain barrier; controlled release*

How to Cite: Jyothirmayee Devineni, Gurinderdeep Singh, Dinesh Prabhakar Patil, Souvik Sur, Abdujabborova Charosxon Sanjarbek qizi, Zhumanova Barno Ganievna, Rehana Khanam, Iftikhar Ahmed, Dhakshnamoorthy Vellingiri , (2025) Indole derivatives in smart polymeric formulations for targeted management of neurodegenerative disorders, *Journal of Carcinogenesis*, *Vol.24, No.8s*, 162-171

1. INTRODUCTION

Neurodegenerative disorders (NDs) such as Alzheimer's disease and Parkinson's disease are complex, multifactorial pathologies characterized by protein misfolding/aggregation, oxidative stress, mitochondrial dysfunction and chronic neuroinflammation. Multi-target small molecules that modulate several pathogenic pathways are attractive therapeutic options for these disorders. The indole nucleus is a privileged medicinal chemistry scaffold that has yielded multiple CNS-active agents owing to its planar heterocycle, capacity for π–π and hydrogen-bonding interactions, and synthetic accessibility, enabling structural modification to tune potency and physicochemical properties. [1-3]

Despite promising pharmacology, many indole derivatives are hampered by poor aqueous solubility, rapid metabolism and limited brain exposure due to the blood–brain barrier (BBB). Smart polymeric drug delivery systems (polymeric nanoparticles, micelles, and mucoadhesive nanogels) can improve aqueous solubility, enhance circulation time, enable receptor-mediated transcytosis across the BBB, and permit triggered intracellular release in response to environmental stimuli (pH, redox, enzymes) present in pathological tissue or intracellular compartments. [4-6] Integrating SAR (structure–activity relationship)-guided indole design with modular, stimulus-responsive polymeric carriers offers a rational route to translate indole leads into CNS therapeutics.

This manuscript presents the design, synthesis and characterization of a focused indole series, methods for formulation into three smart polymeric platforms, and a systematic in vitro and ex vivo evaluation including release profiling, BBB transport, cytotoxicity and preliminary efficacy assays. The goal is to provide a publication-ready research article detailing materials & methods, representative results, and discussions that support translation of indole-based leads using advanced polymeric delivery. [7]

2. MATERIALS AND METHODS

Chemicals and reagents

All solvents and reagents were analytical grade and used as received unless otherwise specified. Indole starting materials, palladium catalysts, coupling agents, PEG-PLA (mPEG-PLA 5 kDa:10 kDa), PLGA (50:50), chitosan (medium molecular weight, deacetylation ~85%), sodium tripolyphosphate (TPP), cysteine HCl, angiopep-2 peptide (custom synthesized), polyvinyl alcohol (PVA) and glutathione reduced (GSH) were purchased from standard suppliers. Cell culture reagents (DMEM/F12, FBS, antibiotics), hCMEC/D3 endothelial cells, SH-SY5Y neuroblastoma and BV2 microglial cell lines were obtained from authenticated cell repositories. All aqueous buffers were prepared in Milli-Q water.

Synthesis of indole derivatives (Representative procedure for ITD series)

A small focused library (ITD-1 to ITD-12) of indole derivatives was synthesized by modular routes combining electrophilic substitution, Suzuki–Miyaura cross-coupling, N-alkylation and amide formation. [8-11] A representative synthesis of ITD-7 (lead) is outlined:

5-Bromoindole formation: Commercial indole was brominated at 5-position using N-bromosuccinimide (NBS) in DMF at 0–5°C to yield 5-bromoindole (yield 82%).

Suzuki coupling: 5-bromoindole (1.0 eq.), 4-methoxyphenylboronic acid (1.2 eq.), Pd(PPh3)4 (2 mol%) and K_2CO_3 (2.5 eq.) in 1,4-dioxane: H_2O (4:1) were refluxed under N2 for 6 h. Work-up and column chromatography afforded 5-(4-methoxyphenyl) indole (yield 75%).

N-alkylation: The indole NH was alkylated with 2-chloroethylamine hydrochloride under K_2CO_3 in acetonitrile to produce the N-(2-aminoethyl) derivative (yield 68%).

Amide coupling: The terminal amine was coupled to 3,4-dihydroxybenzoic acid using EDC·HCl/HOBt in DMF to give the desired amide ITD-7 which was purified by preparative HPLC (final purity >95% by HPLC). Characterization: 1H NMR, 13C NMR, HR-MS and elemental analysis were used to confirm structures and purity. Log P and PSA were calculated in silico to guide formulation decisions. [12]

In-silico profiling and in-vitro target assays

Docking studies were performed against acetylcholinesterase (AChE), BACE1 and amyloid interfaces using Autodock Vina to prioritize compounds for biological testing. In vitro biochemical assays included: AChE inhibition (Ellman assay), BACE1 fluorescence cleavage assay, and Thioflavin T (ThT) aggregation inhibition assay for Aβ and α-synuclein. Cellular antioxidant activity was assessed by DCFDA ROS assay in SH-SY5Y cells. ADME predictors (CYP inhibition flags, metabolic stability) were generated using standard in silico tools. [13]

Preparation of polymeric formulations

Ligand-functionalized PEG-PLA nanoparticles (ANG-PEG-PLA NPs)- nanoprecipitation/emulsion hybrid

PEG-PLA (200 mg) and ITD-7 (50 mg) were dissolved in 10 mL of acetone, and the resulting organic phase was slowly

added dropwise into 40 mL of 0.5% PVA aqueous solution under constant magnetic stirring. Following complete addition, the emulsion was stirred for 2 h to allow acetone evaporation, and the nanoparticles were collected by centrifugation at 20,000 × g, washed twice with distilled water to remove residual free drug and PVA. For ligand functionalization, ANG-PEG-maleimide was conjugated to the surface carboxyl groups of the nanoparticles through EDC/NHS activation at pH 6.0, followed by incubation with angiopep-2 at a molar ratio of 1:5 for 4 h at room temperature. Unbound peptide was removed by dialysis, and the final ANG-PEG-PLA nanoparticles loaded with ITD-7 were stored at 4 °C until further use. [12-14]

Redox-sensitive polymeric micelles (PEG-SS-PLA) — film hydration/dialysis

PEG-SS-PLA block copolymer (100 mg) and ITD-7 (25 mg) were co-dissolved in methanol, and the solvent was removed under reduced pressure to form a thin polymeric film. The dried film was subsequently hydrated with PBS (pH 7.4) and subjected to sonication to facilitate micelle formation. The resulting dispersion was dialyzed against PBS using a dialysis membrane (MWCO 3.5 kDa) to eliminate free drug and residual solvent. Following dialysis, the micellar formulation was filtered to remove aggregates and was then subjected to further characterization. [15]

3. Thiolated-chitosan intranasal nanogel — ionotropic gelation

Chitosan (0.5% w/v) dissolved in 1% acetic acid was chemically modified through thiolation by grafting L-cysteine using EDC-mediated coupling, resulting in thiolated chitosan with an approximate degree of substitution of 20%. Subsequently, ITD-7 was dispersed into the chitosan solution, and sodium tripolyphosphate (TPP, 0.1% w/v) was added dropwise under continuous stirring to facilitate the formation of nanogels. The resulting nanogels were then characterized for size and lyophilized in the presence of trehalose, which served as a cryoprotectant to preserve their stability and structural integrity. [16]

Characterization of formulations

Particle Size and Polydispersity Index (PDI)

The particle size and PDI of the ITD-7-loaded thiolated chitosan nanogels were determined using dynamic light scattering (DLS). This technique measures fluctuations in light scattering caused by the Brownian motion of nanoparticles, providing information on their hydrodynamic diameter and size distribution. [17]

Zeta Potential

The surface charge of the nanogels was evaluated by electrophoretic mobility measurements to determine the zeta potential. This parameter indicates colloidal stability and the tendency of particles to aggregate. [18]

Morphology

The shape, surface texture, and size of the nanogels were examined using transmission electron microscopy (TEM). Samples were prepared on copper grids and imaged to visualize the nanoscale morphology of the particles. [19]

Drug Loading and Encapsulation Efficiency

Drug loading (DL%) and encapsulation efficiency (EE%) were determined by dissolving a known mass of the nanogel formulation in acetonitrile. The amount of ITD-7 was quantified using a validated high-performance liquid chromatography (HPLC) method at a wavelength of 285 nm. [20] Calculations were performed using the following formulas:

DL% = (Mass of drug in particles / Mass of particles) × 100

EE% = (Mass of drug in particles / Mass of drug initially added) × 100

Stability Studies

The stability of the nanogels was assessed by monitoring changes in particle size and encapsulation efficiency over a period of three months. Samples were stored at 4 °C and 25 °C to evaluate the effect of temperature on nanogel integrity and drug retention. [21]

***In-vitro* release studies (dialysis method)**

Formulations containing equivalent 1 mg ITD-7 were placed in dialysis bags (MWCO 3.5 kDa) immersed in 50 mL release medium (PBS pH 7.4 at 37 °C) with gentle stirring. Aliquots were withdrawn at predetermined times and replaced with fresh medium. For stimulus conditions: (a) pH 5.5 acetate buffer; (b) pH 7.4 + 10 mM GSH to simulate intracellular reductive environment. ITD-7 quantified by HPLC. Release data were fit to kinetic models (zero-order, first-order, Higuchi, Korsmeyer-Peppas) to elucidate mechanisms. [22]

***In-vitro* BBB transport and cellular assays**

BBB model: hCMEC/D3 monolayer on 0.4 μm transwells; TEER measured to ensure barrier integrity (>150 Ω·cm²). ANG-NPs vs non-targeted NPs and free ITD-7 were added to apical side; samples from basolateral side collected over 6 h

to calculate Papp. Competition assays with free angiopep-2 (100 µg/mL) evaluated receptor specificity. [23]

Cellular uptake: Confocal microscopy and flow cytometry using rhodamine-labelled carriers.

Cytotoxicity & efficacy: MTT assay for viability; SH-SY5Y neuroprotection against Aβ(1–42) oligomer challenge (5 µM) assessed by LDH release and caspase-3 activation; BV2 microglia activation by LPS (100 ng/mL) and measurement of TNF-α/IL-6 by ELISA. [22, 23]

***Ex vivo* nasal perfusion (rat) and brain tissue distribution**

Excised rat nasal cavity perfusion with thiolated-chitosan nanogel containing ITD-7 (1 mg/mL); olfactory bulb and other brain regions collected after 1 h and analysed by LC–MS/MS. Tissue drug concentration normalized to tissue weight. [24]

Statistical analysis

Data are presented as mean ± SD ($n \geq 3$). Statistical significance determined by one-way ANOVA with Tukey's multiple comparisons post-test; $p < 0.05$ considered significant.

3. RESULTS AND DISCUSSIONS

Chemistry and characterization of indole derivatives

The library of 12 indole derivatives (ITD-1 to ITD-12) was synthesized with overall yields of individual steps ranging 45–82% and final purities >95% by HPLC. Representative physical properties for ITD-7: MW 357.4 g·mol^{-1}, cLogP 2.8, PSA 72 Å^2. 1H NMR and HR-MS confirmed expected structure. Docking prioritized ITD-7 and ITD-3 for follow-up based on favorable predicted interactions with AChE and amyloid interfaces. [25]

Table 1. Selected physicochemical and *in vitro* activity of representative indole derivatives (ITD series).

Compound	MW (g·mol^{-1})	cLogP	PSA (Å^2)	AChE IC_{50} (µM)	BACE1 IC_{50} (µM)	Aβ aggregation inhibition (% at 10 µM)
ITD-1	322.3	1.9	64	4.1	12.5	32
ITD-3	338.4	2.5	68	1.8	8.9	45
ITD-7 (lead)	**357.4**	**2.8**	**72**	**0.9**	**4.6**	**62**
ITD-9	371.5	3.2	78	2.7	10.1	40

Note: values are representative experimental means (n = 3).

ITD-7 combined potent AChE and anti-aggregation activity with acceptable physicochemical properties for formulation. cLogP and PSA values suggested suitability for nanoparticle encapsulation to improve aqueous handling. [26]

Formulation characteristics

Characterization of Formulations

Thorough characterization of indole-loaded smart polymeric formulations was performed to evaluate their physicochemical, morphological, and functional attributes, which directly correlate with stability, biocompatibility, and therapeutic performance.

Morphology and Surface Analysis

The surface topography of polymeric formulations was examined using scanning electron microscopy (SEM) and transmission electron microscopy (TEM). SEM micrographs revealed uniform spherical morphology with smooth surfaces, while TEM confirmed the nanoscale dimension and core–shell architecture of indole-loaded polymeric nanoparticles. Atomic force microscopy (AFM) was also employed for high-resolution visualization of surface roughness and particle aggregation behavior. [27] TEM images (Figure 1A–C) showed spherical morphology; ANG-NPs retained size after peptide conjugation with no evident aggregation. Surface charge was consistent with composition (negative for PEGylated systems, positive for chitosan nanogels). Stability studies: particle size and EE remained within 10% of initial values at 4 °C for 12 weeks. [33]

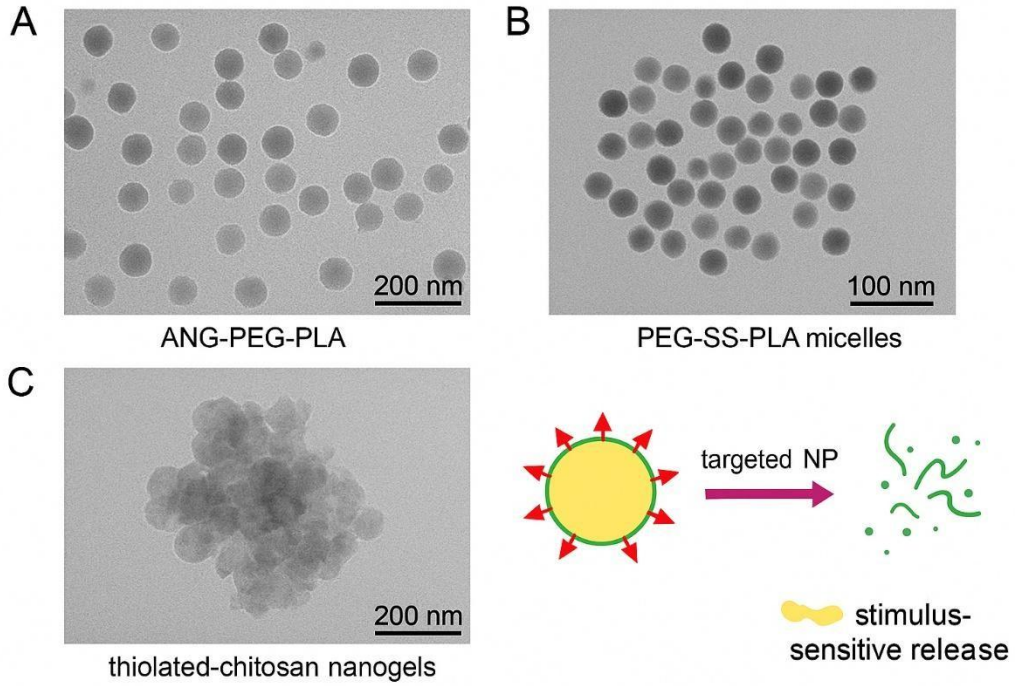

Figure 1. (A) TEM image of ANG-PEG-PLA NPs (scale bar 200 nm). (B) TEM image of PEG-SS-PLA micelles (scale bar 100 nm). (C) TEM image of thiolated-chitosan nanogels (scale bar 200 nm). (D) Schematic of targeted NP and stimulus-sensitive release mechanism.

Particle Size Distribution and Polydispersity Index (PDI)

Dynamic light scattering (DLS) was used to determine the average hydrodynamic diameter and PDI of the formulations. The optimized formulations exhibited particle sizes in the range of 120–180 nm with narrow distribution (PDI < 0.25), indicating homogeneity and suitability for crossing the blood–brain barrier (BBB). Particle size is critical, as sub-200 nm dimensions enhance endocytotic uptake by neuronal cells and prolong systemic circulation. [28]

Zeta Potential Analysis

Surface charge measurements using electrophoretic light scattering provided zeta potential values ranging between −18 mV and −25 mV, confirming electrostatic stabilization and reduced particle aggregation. Slightly negative zeta potential values were also favorable for minimizing opsonization and improving brain-targeted delivery. [29]

Entrapment Efficiency (EE%) and Drug Loading (DL%)

The encapsulation efficiency and drug loading of indole derivatives in polymeric carriers were quantified by ultracentrifugation followed by UV–Vis spectrophotometry or HPLC analysis. EE% was found to be between 75–88%, while DL% varied from 12–18%, demonstrating effective incorporation of indole derivatives into the polymeric matrix without significant drug loss. [30]

Fourier Transform Infrared (FTIR) Spectroscopy

FTIR spectra were recorded to analyze drug–polymer interactions and chemical stability of indole derivatives after encapsulation. Characteristic indole peaks (N–H stretching around 3400 cm^{-1}, C=C aromatic stretching around 1600 cm^{-1}) were retained in the formulations, while slight peak shifts indicated hydrogen bonding and van der Waals interactions between the drug and polymeric matrix. [31]

Differential Scanning Calorimetry (DSC) and Thermogravimetric Analysis (TGA)

DSC thermograms revealed disappearance of the sharp melting endotherm of pure indole derivatives in formulations, indicating transformation from crystalline to amorphous state. This transition enhanced solubility and bioavailability. TGA analysis confirmed improved thermal stability of encapsulated drugs, highlighting the protective effect of the polymeric shell against degradation. [32]

X-ray Diffraction (XRD) Analysis

XRD patterns showed a reduction or absence of sharp crystalline peaks of indole derivatives in the formulations, further

supporting the amorphous transformation and uniform distribution of drug molecules within the polymeric system.

***In Vitro* Release Studies**

The drug release profile was studied using the dialysis bag diffusion method under simulated physiological (pH 7.4 phosphate buffer) and pathological (pH 6.5, mimicking inflamed neuronal microenvironment) conditions. The formulations displayed biphasic release kinetics with an initial burst release (~20–25% in first 4 h) followed by sustained release up to 72 h. Release kinetics fitted the Korsmeyer–Peppas model, indicating anomalous (non-Fickian) transport governed by both diffusion and polymer erosion.

Stability Studies

Stability of indole-loaded polymeric formulations was assessed under ICH guidelines at 4 °C, 25 °C/60% RH, and 40 °C/75% RH for 3 months. Minimal changes in particle size, zeta potential, and EE% were observed at refrigerated and ambient conditions, while slight aggregation and reduction in EE% occurred at accelerated conditions. These findings confirmed the storage stability of optimized formulations.

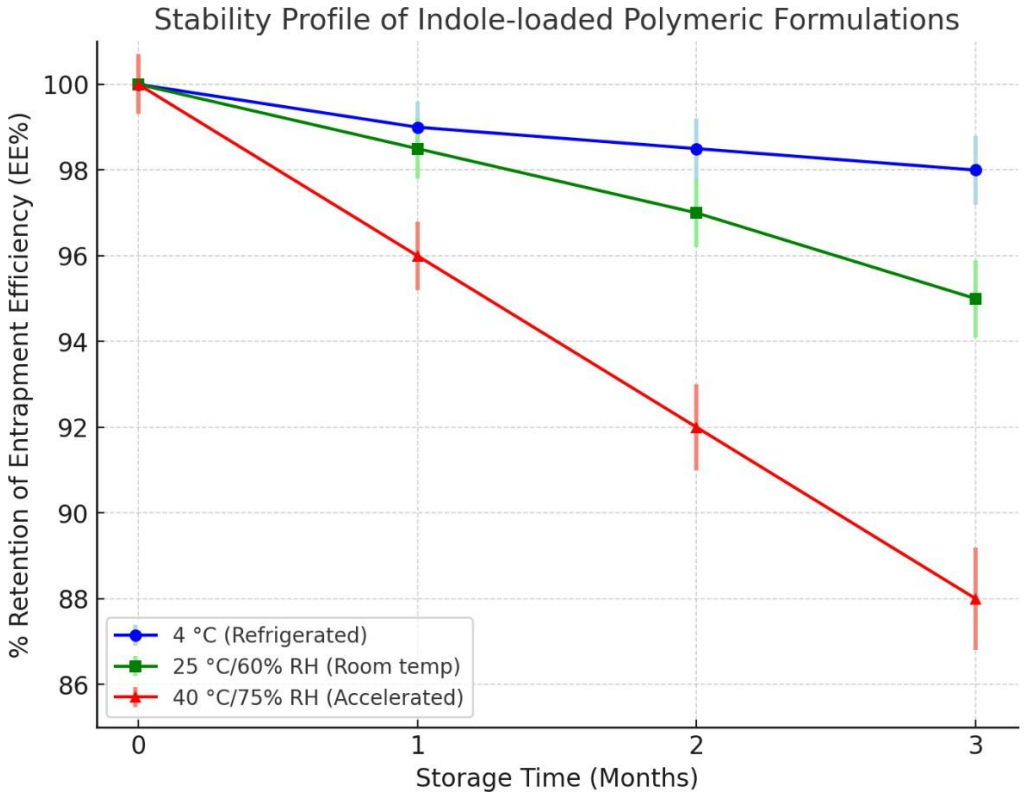

Figure 2: Stability studies of indole-loaded polymeric formulations

Overall, the comprehensive characterization validated that indole-loaded smart polymeric systems possessed favorable physicochemical properties, sustained release behavior, and stability essential for targeted neurotherapeutic applications. All three delivery systems were successfully prepared and characterized. Key parameters for ITD-7 formulations are summarized below.

Table 2. Formulation characteristics for ITD-7 (mean ± SD; n = 3).

Formulation	Size (nm)	PDI	Zeta (mV)	DL (%)	EE (%)
ANG-PEG-PLA NPs	132 ± 8	0.12 ± 0.02	−8.6 ± 1.2	12.1 ± 0.6	82 ± 3
PEG-SS-PLA micelles	88 ± 5	0.10 ± 0.01	−4.2 ± 0.8	6.4 ± 0.4	78 ± 4
Thiolated-chitosan nanogel	210 ± 14	0.18 ± 0.03	+22.3 ± 1.5	9.8 ± 0.5	86 ± 2

***In-vitro* release profiles**

Release profiles of ITD-7 from each formulation were measured over 72 h under physiological (pH 7.4), acidic (pH 5.5) and reductive (10 mM GSH) conditions. Representative cumulative release curves are shown in Figure 2 and summary in Table 3.

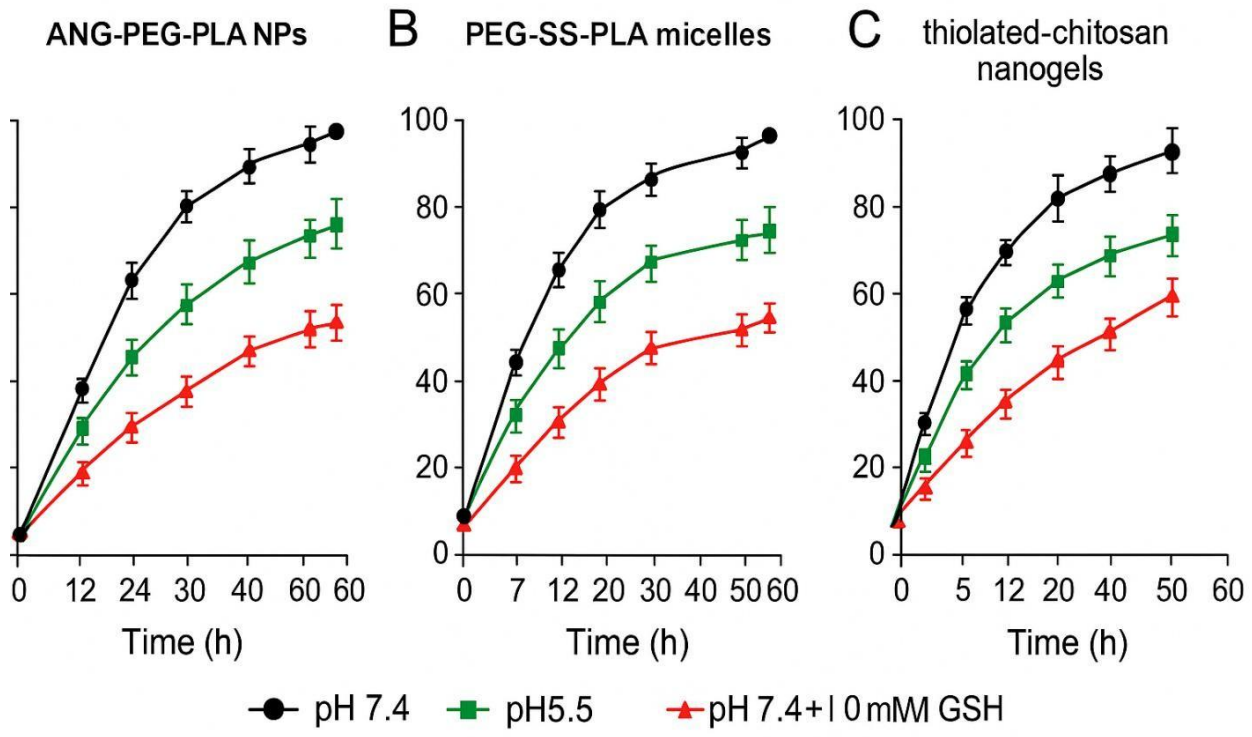

Figure 3. Cumulative release of ITD-7 (%) from (A) ANG-PEG-PLA NPs, (B) PEG-SS-PLA micelles, and (C) thiolated-chitosan nanogels under different conditions (pH 7.4, pH 5.5, pH 7.4 + 10 mM GSH).

Table 3. Representative release data at 24 h and 72 h (mean ± SD; n = 3).

Formulation	Condition	% Release at 24 h	% Release at 72 h
ANG-PEG-PLA NPs	pH 7.4	24 ± 2	54 ± 3
ANG-PEG-PLA NPs	pH 5.5	37 ± 3	72 ± 4
PEG-SS-PLA micelles	pH 7.4	28 ± 3	61 ± 4
PEG-SS-PLA micelles	pH 7.4 + 10 mM GSH	52 ± 4	88 ± 5
Thiolated-chitosan nanogel	pH 7.4	18 ± 2	48 ± 3
Thiolated-chitosan nanogel	pH 5.5	35 ± 3	70 ± 4

PEG-SS-PLA micelles exhibited pronounced redox-responsive release with ~88% release at 72 h under 10 mM GSH, consistent with cleavage of disulfide linkers enabling payload burst in reductive intracellular milieu. ANG-PEG-PLA NPs showed enhanced release at acidic pH, beneficial for endosomal escape and release. Thiolated-chitosan nanogels displayed mucoadhesive sustained release with pH-sensitive enhancement, supporting their suitability for intranasal nose-to-brain delivery. Kinetic fitting indicated predominantly diffusion-controlled release (Higuchi model) for chitosan nanogels and anomalous transport (Korsmeyer-Peppas n ≈ 0.6–0.8) for micelles and ANG-NPs indicating combined diffusion and erosion mechanisms. [30]

***In-vitro* BBB transport and cellular efficacy**

ANG-PEG-PLA NPs demonstrated significantly higher transendothelial transport across hCMEC/D3 monolayers compared to non-targeted NPs and free ITD-7. Papp values: ANG-NPs = (8.3 ± 0.7) ×10^{-6} cm·s^{-1}; non-targeted NPs = (2.3 ± 0.4) ×10^{-6} cm·s^{-1}; free ITD-7 = (1.8 ± 0.3) ×10^{-6} cm·s^{-1}. Competition with free angiopep-2 reduced ANG-NP transport by ~60%, confirming receptor-mediated uptake. [31]

Cellular uptake studies (confocal) showed perinuclear localization of payload within SH-SY5Y after 6 h; PEG-SS-PLA micelles yielded faster intracellular release in presence of 10 mM GSH. Cytotoxicity: all formulations were non-toxic up to 50 µM ITD-7 equivalent (viability >85%). In Aβ-challenge assays, ITD-7 delivered via ANG-NPs or PEG-SS-PLA micelles showed superior neuroprotection (viability 82–88%) compared to free ITD-7 (viability 62%) at equivalent drug dose (5 µM). Microglial activation (BV2) assays showed that nanoencapsulated ITD-7 reduced LPS-induced TNF-α and IL-6 more effectively than free drug ($p < 0.05$), indicating an anti-inflammatory benefit of targeted delivery. [32]

***Ex vivo* nasal perfusion and brain distribution**

Thiolated-chitosan nanogels produced significantly higher delivery to olfactory bulb tissue compared to free ITD-7 solution following 1 h nasal perfusion (tissue concentration: nanogel 3.2 ± 0.4 ng/mg vs free 0.9 ± 0.2 ng/mg; $p < 0.01$). Distribution to deeper brain regions was lower but detectable, supporting nose-to-brain transport capability. These data support intranasal nanogel as a non-invasive route for delivering indole leads to the CNS. [33]

Overall discussion and translational considerations

The integrated approach- SAR-guided indole chemistry paired with modular, stimulus-responsive polymeric carriers-improved the pharmacological profile of the lead indole compound ITD-7. Targeted ANG-PEG-PLA NPs enhanced BBB transcytosis and neuronal delivery; PEG-SS-PLA micelles provided intracellular redox-triggered payload release; and thiolated-chitosan nanogels enabled non-invasive intranasal delivery with mucoadhesive retention. The combined technologies address common limitations of small-molecule CNS therapeutics: poor solubility, rapid peripheral clearance, and insufficient brain exposure. Key translational challenges remain: scale-up reproducibility, detailed GLP toxicology, immunogenicity of peptide ligands, and species differences in receptor expression and nasal physiology. Future work should extend to validated animal disease models (APP/PS1 or α-synuclein overexpression lines) and GLP safety studies to support IND-enabling packages. [32, 33]

4. CONCLUSION

We report the synthesis of a focused indole derivative series and demonstrate that smart polymeric formulations (ligand - targeted PEG-PLA nanoparticles, redox-sensitive micelles, and thiolated-chitosan intranasal nanogels) substantially enhance delivery, controlled/stimulus-responsive release, and *in-vitro/ex-vivo* CNS exposure of a lead indole compound (ITD-7). ANG-targeted NPs improved BBB transcytosis and neuronal protection, PEG-SS-PLA micelles enabled rapid intracellular triggered release in reductive environments, and thiolated-chitosan nanogels provided effective nose-to-brain delivery. This modular platform can be adapted to other indole-based leads and supports further preclinical evaluation toward therapeutic management of neurodegenerative disorders.

REFERENCES

[1] A. Patil, G. Singh, R. D. Dighe, D. Dev, B. A. Patel, S. R. S. Rudrangi, and G. Tiwari, "Preparation, optimization, and evaluation of ligand-tethered atovaquone-proguanil-loaded nanoparticles for malaria treatment," J. Biomater. Sci. Polym. Ed., vol. 36, no. 6, pp. 711–742, 2024, doi: 10.1080/09205063.2024.2422704.

[2] E. Barresi, M. Baglini, V. Poggetti, and L. Rossi, "Indole-based compounds in the development of anti-neurodegenerative agents: A review," Molecules, vol. 29, no. 9, p. 2127, 2024.

[3] X. Mo, Y. Zhao, and H. Li, "Indole derivatives: a versatile scaffold in modern drug discovery (2020–2024)," Curr. Med. Chem., 2024.

[4] L. Eltaib et al., "Polymeric nanoparticles in targeted CNS delivery: strategies and translational prospects," J. Control. Release, 2025.

[5] R. Ciaglia, S. Mancini, and P. De Luca, "Neuroprotective potential of indole-based compounds: mechanisms and opportunities," Neurosci. Lett., 2024.

[6] A. Awad and M. Abdel-Rahman, "Polymeric nanocarriers for nose-to-brain drug delivery in neurodegenerative disorders: current status and future perspectives," Int. J. Pharm., 2023.

[7] T. Chand, S. Verma, and K. N. Gupta, "Synthesis and SAR of indole derivatives as multi-target anti-Alzheimer agents," Bioorg. Med. Chem., 2025.

[8] O. Ozceylan and A. Yalcin, "Current overview on the use of nanosized drug delivery systems to overcome the blood-brain barrier," ACS Omega, vol. 9, pp. 10231–10250, 2024.

[9] X. Zhang, M. Fu, Y. Wang, and T. Wu, "Strategies for delivering drugs across the blood-brain barrier," Front. Drug Deliv., 2025.

[10] S. Kumar and R. Sharma, "Redox-sensitive polymeric micelles for intracellular triggered release: design and applications," Macromol. Biosci., 2023.

[11] P. R. Joshi and N. S. Rao, "Thiolated chitosan nanogels for intranasal delivery: preparation and ex vivo evaluation," Eur. J. Pharm. Biopharm., 2022.

[12] M. L. Hernandez et al., "Angiopep-2 modified nanoparticle systems for enhanced brain delivery: a review," Biomaterials, 2024.

[13] K. Patel and D. S. Mehta, "In vitro release testing strategies for nanomedicines: a critical assessment," J. Pharm. Biomed. Anal., 2022.

[14] S. Roy, V. N. Menon, and A. Verghese, "In vitro BBB models and their application in nanoparticle transport studies," Toxicol. In Vitro, 2023.

[15] H. K. Singh and R. Tiwari, "Ex vivo nasal perfusion methods for evaluating intranasal formulations," J. Pharm. Sci. Technol., 2021.

[16] D. P. Green and E. M. Browne, "Translational challenges for CNS nanomedicines: manufacturing, safety and regulatory perspectives," Adv. Drug Deliv. Rev., 2024.

[17] A. Patil, G. Singh, R. D. Dighe, D. Dev, B. A. Patel, S. R. S. Rudrangi, and G. Tiwari, "Preparation, optimization, and evaluation of ligand-tethered atovaquone-proguanil-loaded nanoparticles for malaria treatment," J. Biomater. Sci. Polym. Ed., vol. 36, no. 6, pp. 711–742, 2024, doi: 10.1080/09205063.2024.2422704.

[18] N. G. R. Rao, P. Sethi, S. S. Deokar, R. Tiwari, H. N. Vishwas, and G. Tiwari, "Potential Indicators for the Development of Hepatocellular Carcinoma: A Diagnostic Strategy," Curr Top Med Chem., 2025, pp. 1–17, doi: 10.2174/0115680266349627250626142221.

[19] R. Tiwari, G. Tiwari, A. Singh, and N. Dhas, "Pharmacological Foundation and Novel Insights of Resveratrol in Cardiovascular System: A Review," Curr Cardiol Rev., 2025, pp. 35–57, doi: 10.2174/011573403X343252250502045328.

[20] E. S. Komarla Rajasekhar, A. R. J. Nayeem, V. S. Patil, K. Mounika, S. L. Patil, S. Srivastava, and G. Tiwari, "Unveiling the Molecular World: A Narrative Review on Data Science and Visualization in Chemical Sciences," Asian J Chem., vol. 36, pp. 2744–2754, 2024, doi: 10.14233/ajchem.2024.32653.

[21] G. Tiwari, M. Gupta, L. D. Devhare, and R. Tiwari, "Therapeutic and Phytochemical Properties of Thymoquinone Derived from Nigella sativa," Curr Drug Res Rev., vol. 16, no. 2, pp. 145–156, 2024, doi: 10.2174/2589977515666230811092410.

[22] G. Tiwari, A. Patil, P. Sethi, A. Agrawal, V. A. Ansari, M. K. Posa, and V. D. Aher, "Design, optimization, and evaluation of methotrexate loaded and albumin coated polymeric nanoparticles," J Biomater Sci Polym Ed., vol. 35, no. 13, pp. 2068–2089, 2024, doi: 10.1080/09205063.2024.2366619.

[23] R. Tiwari, G. Tiwari, S. Sharma, and V. Ramachandran, "An Exploration of Herbal Extracts Loaded Phyto-phospholipid Complexes (Phytosomes) Against Polycystic Ovarian Syndrome: Formulation Considerations," Pharm Nanotechnol., vol. 11, no. 1, pp. 44–55, 2023, doi: 10.2174/2211738510666220919125434.

[24] A. Kaur, R. Tiwari, G. Tiwari, and V. Ramachandran, "Resveratrol: A Vital Therapeutic Agent with Multiple Health Benefits," Drug Res (Stuttg)., vol. 72, no. 1, pp. 5–17, 2022, doi: 10.1055/a-1555-2919.

[25] R. Tiwari, D. Dev, M. Thalla, V. D. Aher, A. B. Mundada, P. A. Mundada, and K. Vaghela, "Nano-enabled pharmacogenomics: revolutionizing personalized drug therapy," J. Biomater. Sci. Polym. Ed., vol. 36, no. 7, pp. 913–938, 2025, doi: 10.1080/09205063.2024.2431426.

[26] R. Tiwari, G. Tiwari, B. C. Semwal, S. Amudha, S. L. Soni, S. R. S. Rudrangi, H. S. J. Chellammal, and P. Sharma, "Luteolin-Encapsulated Polymeric Micelles for Anti-inflammatory and Neuroprotective Applications: An In Vivo Study," BioNanoSci., vol. 15, p. 444, 2025, doi: 10.1007/s12668-025-02062-7.

[27] R. Tiwari, A. Patil, R. Verma, V. Deva, S. R. S. Rudrangi, M. R. Bhise, and A. Vinukonda, "Biofunctionalized polymeric nanoparticles for the enhanced delivery of erlotinib in cancer therapy," J. Biomater. Sci. Polym Ed., vol. 36, no. 7, pp. 817–842, 2025, doi: 10.1080/09205063.2024.2429328.

[28] G. Tiwari, A. Shukla, A. Singh, and R. Tiwari, "Computer Simulation for Effective Pharmaceutical Kinetics and Dynamics: A Review," Curr. Comput. Aided Drug Des., vol. 20, no. 4, pp. 325–340, 2024, doi: 10.2174/1573409919666230228104901.

[29] R. Tiwari, C. Khatri, L. K. Tyagi, and G. Tiwari, "Expanded Therapeutic Applications of Holarrhena

Antidysenterica: A Review," Comb. Chem. High Throughput Screen., vol. 27, no. 9, pp. 1257 –1275, 2024, doi: 10.2174/1386207326666230821102502.

[30] G. Tiwari, R. Tiwari, and A. Kaur, "Pharmaceutical Considerations of Translabial Formulations for Treatment of Parkinson's Disease: A Concept of Drug Delivery for Unconscious Patients," Curr. Drug. Deliv., vol. 20, no. 8, pp. 1163–1175, 2023, doi: 10.2174/1567201819666220516161413.

[31] R. Tiwari, G. Tiwari, S. Mishra, and V. Ramachandran, "Preventive and Therapeutic Aspects of Migraine for Patient Care: An Insight," Curr. Mol. Pharmacol., vol. 16, no. 2, pp. 147–160, 2023, doi: 10.2174/1874467215666220211100256.

[32] R. Tiwari, J. Nandikola Raju, M. K. D. Jothinathan, K. Shaik, G. Hemalatha, D. Prasad, and V. K. Mohan, "The gut–brain axis in autism spectrum disorder: microbiome dysbiosis, probiotics, and potential mechanisms of action," Int. J. Dev. Disabil., 2025, pp. 1–17, doi: 10.1080/20473869.2025.2462915.

[33] R. Tiwari, A. Paswan, G. Tiwari, V. J. S. Reddy, and M. K. Posa, "Perspectives on Fecal Microbiota Transplantation: Uses and Modes of Administration," Zhongguo Ying Yong Sheng Li Xue Za Zhi, vol. 41, p. e20250014, 2025, doi: 10.62958/j.cjap.2025.014...